ELECTRON BEAM WELDING OF TITANIUM AND ALUMINUM ALLOYS WITH A VANADIUM FILLER

Georgi Kotlarski[1,2], Darina Kaisheva[1,3], Dimitar Dechev[1], Nikolay Ivanov[1], Maria Ormanova[1,2,4], Vladimir Dunchev[2,5], Angel Anchev[2,5], Borislav Stoyanov[2,6], Stefan Valkov[1,2,4]

[1]*Institute of Electronics, Bulgarian Academy of Sciences*
72 Tsarigradsko Chausse Blvd.,
Sofia 1784, Bulgaria, gvkotlarski@gmail.com (G.K.);
dadechev@abv.bg (D.D); n_ivanov@ie.bas.bg (N.I);
stsvalkov@gmail.com (S.V.)
[2]*Center of competence "Smart mechatronic, eco-and energy-saving systems and technologies", 5 Doctor Iliev Detskia St.,*
Gabrovo 5300, Bulgaria, v.dunchev@tugab.bg (V.D.)
[3]*Department of Mathematics and Physics, Neofit Rilski South-West University*
66 Ivan Michailov St., Blagoevgrad 2700, Bulgaria, darinakaisheva@abv.bg (D.K.)
[4]*Department of Mathematics, Informatics and Natural Sciences*
Technical University of Gabrovo, 4 H. Dimitar St.,
Gabrovo 5300, Bulgaria, m.ormanova@ie.bas.bg (M.O.)
[5]*Department of Material Science and Mechanics of Materials*
Technical University of Gabrovo, 4 H. Dimitar St.,
Gabrovo 5300, Bulgaria, anchev@tugab.bg (A.A.)
[6]*Department of Industrial Design and Textile Engineering*
Technical University of Gabrovo, 4 H. Dimitar St.,
Gabrovo 5300, Bulgaria; stoyanov_b@mail.bg (B.S.)

Received 25 August 2025
Accepted 13 December 2025 *DOI: 10.59957/jctm.v61.i2.2026.18*

ABSTRACT

This work demonstrates the influence of using a V filler as an intermediate layer between Ti_6Al_4V and Al6082T6 plates. The study focuses on the microstructure and some mechanical properties of the weld seams created by electron beam welding. The microstructure of the specimens was examined by X-ray diffraction (XRD), scanning electron microscopy (SEM), and energy-dispersive X-ray spectroscopy (EDS) analyses. The study measured microhardness and tensile properties of the samples. A weld seam rich in titanium was formed. This resulted in the presence of γ-TiAl (L10) and α_2-Ti_3Al (D019) intermetallic phases. Using the V interlayer improved the distribution of Ti-Al intermetallic in the fusion zone. The microhardness of the samples did not change substantially with the addition of a V interlayer. In the fusion zone, it was 537 ± 43 HV0.05. With a V layer, it was 548 ± 50 HV0.05. However, tensile properties showed a slight increase. The sample without a filler had an ultimate tensile strength of 45 ± 6 MPa. With a V filler, it increased to 71 ± 11 MPa. This work proves that using V as an interlayer between Ti64 and Al6082T6 alloys is feasible for improving the structure and some mechanical properties. However, future studies are needed to optimize the V integration procedure.

Keywords: electron beam welding, vanadium interlayer, magnetron sputtering, titanium alloy, aluminum alloy.

INTRODUCTION

In the last few decades with the advanced research and development of alloys a new possibility of manufacturing lightweight components with a high strength was investigated and materials such as aluminium alloys dominated the market [1 - 3]. Aluminium alloys are light, have good corrosion resistance, good thermal and

electrical conductivities, high strength, good ductility and formability, etc. In search of new strong, lightweight materials the scientific community has come up with a solution in the form of titanium alloys such as Ti5Al4, Ti6Al4, and others. They have excellent applicability in several sectors due to their incredibly high strength, lightweight, good corrosion resistance [4 - 6]. Titanium and its alloys cost significantly more than conventional materials such as steel and aluminium, which means their application needs to be very well though-out and economically viable. Due to this, a possible solution to this problem is the formation of non-detachable joints between titanium and its alloys with other materials. This not only decreases the materials costs but also allows to combine the properties of at least two, or more different metals and alloys and improves the versatility of the materials' applications.

The formation of non-detachable joints can be performed in a multitude of ways, but the most common one is welding. A large array of welding techniques exists and are used in practice such as gas metal arc welding (GMAW), gas tungsten arc welding (GTAW), friction stir welding (FSW), laser beam welding (LBW), diffusion welding (DW), electron beam welding (EBW), and more. Friction stir welding is a highly popular method that has been the object of investigations due to the excellent intermetallic formation control of the process. Laser beam welding and electron beam welding have also been investigated due to their advantages over other methods such as the high precision, easy automation, high efficiency, and in the case of EBW the presence of a high-vacuum environment. The last two methods, particularly electron beam welding, allow for the formation of deep weld seams without the necessity of forming V grooves. This means that EBW and LBW are particularly valuable when it comes to welding highly specific objects and are also ideal for the formation of butt joints.

There are, however, some well-known issues regarding the welding of titanium alloys and aluminium alloys, the most common one being the formation of intermetallic phases (mostly binary). This has been reported by several authors and can occur during all types of welding. In the case of LBW and EBW, though it is particularly easy to achieve due to the high melting-cooling speeds, which are a prerequisite for the formation of intermetallic compounds (IMCs) [7].

To mitigate the issue, the application of fillers has been suggested by previous researchers. AlSi12 fillers have been applied previously to moderate the formation of the typical brittle binary intermetallic compounds such as $TiAl_3$, Ti_3Al, TiAl, and others [8, 9]. Their results show excellent achievements both from structural and mechanical points of view. The application of such a filler reportedly leads to the formation of ternary Ti-Al-Si phases that are not only not as brittle as the binary Ti-Al ones but also hinder the formation of the last.

An interesting and promising material that can be used as a filler interlayer is vanadium. It is known to have great application in the preparation of ($\alpha + \beta$) Ti alloys, as a β phase stabilizer. Typical examples of such alloys are Ti3Al2.5V, Ti5Al4V, Ti6Al4V, etc. Aluminium is typically used as an α phase moderator. Typically, the last suffices for the strength of the alloy, whereas the β stabilizer ensures the plasticity of the alloy. It is possible that during the process of welding the additional quantity of vanadium to increase the plasticity of the weld seam. Additionally, vanadium is a highly non-thermally conductive material, meaning that theoretical change of the heat distribution process is expected. This would also achieve interesting results.

Due to the high potential of vanadium as a filler material and the almost non-existent previous research regarding its application the current study aims to investigate the effect of applying a V filler during the process of electron beam welding of titanium and aluminium alloys on the output structure and some mechanical properties of the weld seams. The results are discussed regarding future application of such interlayers.

EXPERIMENTAL

To this work ASTM Grade 5 Ti-6Al-4V (Ti64), and EN AW-6082 T6 (Al6082T6) were selected as the dissimilar alloys. The nominal chemical composition of the alloys, as provided from the manufacturer, is summarized in Table 1.

The as-delivered materials were in the form of metal plates with dimensions of 100 x 50 x 8 mm. Prior to the welding process their surfaces were computer numerical control (CNC) machined to minimize the distance between them and assure a clean surface with minimal (idealistically none) contaminants.

Table 1. Nominal chemical composition of the used alloys.

Alloy	Chemical composition, wt. %						
	Fe	V	Al	Ti	Si	Mn	Mg
Ti6Al4V	0.3	3.5 - 4.5	5.5 - 6.5	bal.	-	-	-
Al6082T6	0.5	-	bal.	-	0.7 - 1.3	0.4 - 1.0	0.6 - 1.2

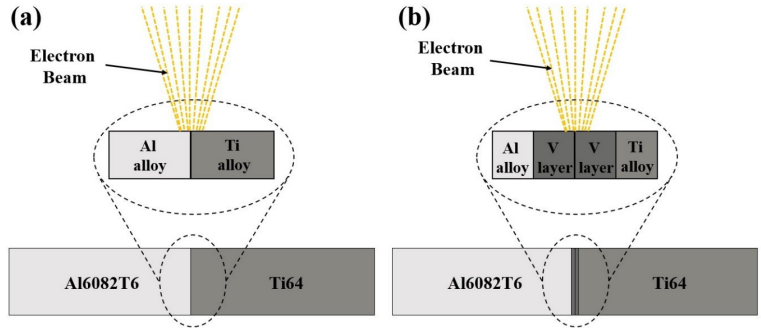

Fig. 1. Schematic of the EBW process without a filler (a), and with a V filler (b).

A vanadium filler was formed atop the cross-sectional surfaces of the welded Ti64 and Al6082T6 plates using a direct current (DC) magnetron sputtering technique. To this a vanadium sputtering target was used with a 99.9 % purity. The surfaces of the plates were cleaned with 99 % isopropyl alcohol, and after placed in the vacuum chamber ion-sputter cleaned for 10 min, which guarantees the purity of the surface prior to the deposition process. The vanadium layer was formed atop the substrates using the following technological conditions: discharge voltage - 460 V; current - 1 A; working pressure - 6.10^{-2} Pa; deposition time - 150 min; layer thickness - approx. 7 µm. After the sputtering process the samples were left in the vacuum chamber in a high vacuum environment to gradually cool down before extracting them from the chamber. The technological conditions of the sputtering process are a result of several previous investigations where V coatings and thin films were formed atop different substrates [10]. The thickness of the formed layers was determined using a weight gain method, where the samples were measured before and after the deposition process using an analytical scale KERN ACJ 200-4M with a range of up to 220 ± 0.0001 g.

The electron beam welding process was performed by joining the cross-sectional surfaces of the specimens together with a mechanical vice to minimize the distance between the surfaces. A weld joint between standard Al6082T6 and Ti64 plates without a filler was performed as a control. In Fig. 1a a schematic of the EBW process of the alloys without a filler is shown, and in Fig. 1b a schematic of the same process is shown, however, with the addition of the vanadium filler. The same technological conditions of electron beam welding were applied in both cases and were as follows: accelerating voltage - 60 kV; beam current - 35 mA; welding speed - 10 mm s^{-1}; circular beam oscillation radius - 0.2 mm; chamber pressure - 5.10^{-2} Pa; focal point size - 200 µm; no offset. The linear heat input during the process was calculated using the relation between the input power P [W] and the speed of welding v [mm s^{-1}] - P/v [J mm^{-1}]. The results indicate a 210 J mm^{-1} heat input.

Metallographic samples were prepared from each welded specimen to study the microstructure of the weld seams. The samples were ground using abrasive paper starting from P220 and ending at P4000. After this the surfaces of the samples were chemically etched using a 10 % solution of HF acid, and then a solution consisting of 2.0 mL HNO_3 and 1.5 mL dH_2O. The same samples were after that used to measure the microhardness. Special hourglass-shaped tensile specimens were made

from the welded specimens. Details about the shape and dimensions of the tensile samples can be found in [11].

X-ray diffraction experiments were performed for phase analysis evaluation using CuKα radiation with a wavelength of 0.154 nm. All experiments were performed using the symmetrical Bragg-Brentano mode at the 2θ scale from 30 to 60° with a step of 0.1° and a count time of 1 s per step.

The microstructure of the samples was investigated using a scanning electron microscope Tescan LYRA3 using a voltage of 20 kV in the back-scattered electrons (BSE) mode. The microscope was equipped with a special attachment, allowing it to perform energy-dispersive X-ray spectroscopy (EDS) analysis.

The microhardness of the samples was determined by performing at least 10 consecutive measurements starting from the aluminium alloy plate going towards the Ti64 one. A test load of 0.49 N was used in all cases. The analysis was performed according to the ISO 6507-1:2018 standard for Vickers hardness testing of metallic samples. The indentations were kept at a minimum distance equal to three times the diameter of the imprints. A dwell time of 10 s was used in all cases.

Three tensile specimens of each sample were tested using a Vibrophore 100 testing machine. The experiments were carried out according to the ISO 6892-1:2019 standard, method B. A static stress-strain rate of 30 MPa s^{-1} was applied. The temperature of measurement was in the range of 10°C to 35°C as per the standard. All fractures of the samples occurred at the border between the fusion and the heat affected zones.

RESULTS AND DISCUSSION

The phase composition of the obtained weld seams was investigated by X-ray diffraction. The results are presented in Fig. 2. All phases were identified using the International Centre for Diffraction Data (ICDD) database, PDFs #441294 for Ti; #040787 for Al; #050678 for TiAl; #371449 for $TiAl_3$; #140451 for Ti_3Al. The XRD pattern of the welded seam formed between the Al6082T6 and Ti64 plates without a filler includes diffraction maxima corresponding to five different phases, namely Ti, Al, TiAl, $TiAl_3$, and Ti_3Al, as shown in Fig. 2a. It is important to note that some amount of vanadium typically is present in the volume of the Ti64 alloy, however, its concentration is noticeably low, due

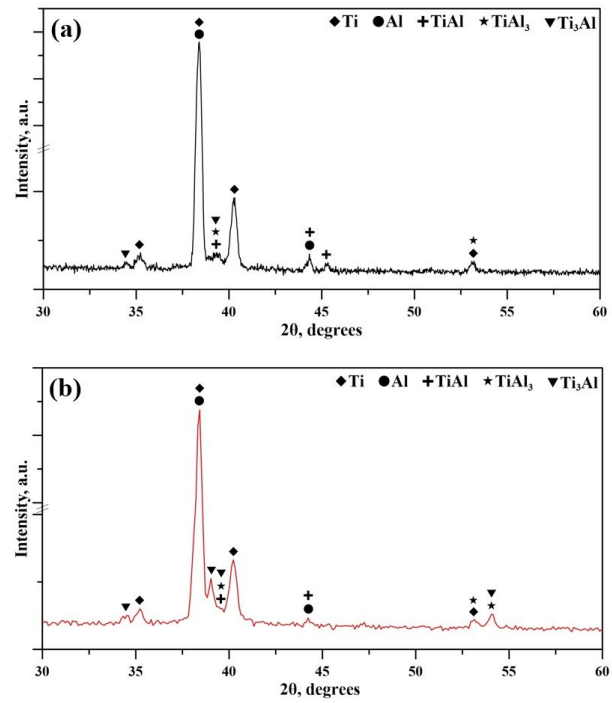

Fig. 2. XRD results of the samples prepared: (a) without a filler, and (b) with a V filler.

to which it completely dissolves into the formed solid solution and because of this no phases corresponding to this element were detected [12]. The presence of binary Ti-Al intermetallic phases is a common occurrence when welding of titanium and aluminium alloys is concerned [13]. Those phases have low free surface energies of formation, which is why they form preferentially compared to others [14]. Along with this they are also well-known for their chemical and thermal stability [15]. The diffraction pattern of the sample prepared with the V filler is shown in Fig. 2b. Evidently, diffraction maxima of the same single and intermetallic phases were present. However, additional peaks of the Ti_3Al at 39.0°, $TiAl_3$ and Ti_3Al at 54.1° phases were detected. Additionally, a single diffraction maximum at 45.2° corresponding to the TiAl phase that was present in the control disappeared after applying the V filler. This results suggests that more Ti was introduced into the weld seam in the case of applying a V filler inducing the formation of a higher concentration of intermetallic phases, however, the intermetallic phases in this case were predominantly Ti_3Al and $TiAl_3$, not only since they have a lower free surface energy of formation compared to TiAl, but also

because of better mixing between the metallic elements during the welding process [14]. This is a hypothesis since a higher concentration of input materials introduces more energy into the weld seam, which energetically, as mentioned, is most favourable to form more stable bonds, which disperse the input energy more efficiently. A similar result was observed by Gadakh et al. [16].

In Fig. 3 SEM images of the weld seam and its sections at different magnifications of the sample prepared without a filler are presented. As it can be seen from Fig. 3a, the shape of the seam is rectangular. No macroscopic pores are visible. Fig. 3b shows a zoomed image of the fusion zone with its boundaries, and heat-affected zones on both sides. A clear mixture between the Ti and Al alloys is visible, which presumably consists of intermetallic compounds, along with potentially pure Al and Ti phases. When studying the Al6082T6 side of the sample, as shown in Fig. 3c, a clear formation of micro-pores with an irregular shape can be seen, which is typical for welding processes of aluminium alloys [17]. Investigating the border between the Al alloy and the fusion zone reveals the presence of long longitudinal cracks. Large transverse cracks along the entire width of the weld seam were also observed when viewing the image presented in Fig. 3c. The presence of these cracks is associated with the large temperature gradients and high cooling rates characteristic of the electron beam welding process along with the significantly different thermophysical properties not only of the Ti and Al phases, but the intermetallic phases as well, that have potentially formed during the process. The distribution of said intermetallic phases in the fusion zone is very clearly visible in Figs 3b and 3e. Evidently, the mixture between the two primary phases of the alloys, namely the Ti, and the Al ones, is not well-propagated. Clear zones where the microstructure of the weld seam changes appear along the entire visible area of the sample. Studying the area shown in Fig. 3f some well-visible martensitic structures can be seen in the structure of the Ti64 plate.

To verify the speculated by the SEM results distribution of the metallic and intermetallic phases an EDS analysis was performed, the results of which are summarized in Table 2. A small area (point) of the each microstructural object of interest were investigated as shown in Figs. 3c, 3e, and 3f. Point 1 is located in the Al6082T6 HAZ and is comprised of 97.86 ± 4.2 at. % of Al. Point 2 corresponds to a similar area, which is why a similar result as in Point 1 was obtained with a composition of 97.86 ± 4.2 at. % Al. The chemical composition of points 3 to 7 clearly indicates the presence of the intermetallic compound TiAl. In these

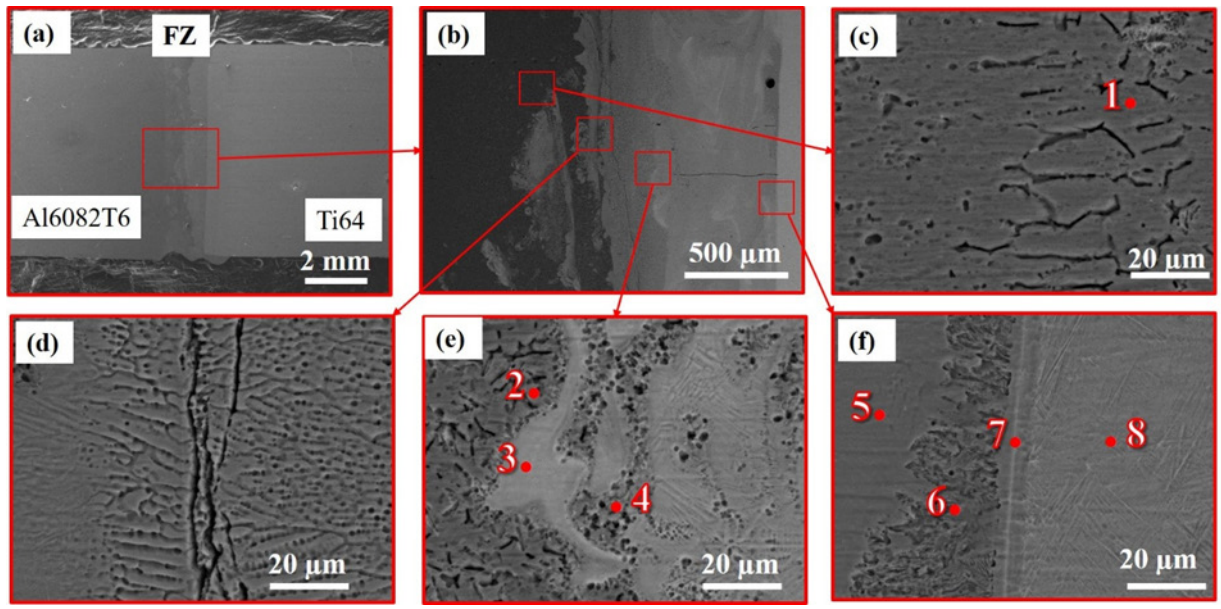

Fig. 3. SEM of the sample prepared without filler: (a) a macro image of the weld seam, (b) a zoomed image of the fusion zone, (c) microstructure of the aluminium HAZ, (d) microstructure of the border between the aluminium HAZ and the FZ, (e) zoomed image of the microstructure of FZ, (f) microstructure of the area at the border between the FZ and the Ti64 HAZ.

Table 2. EDS results for the control sample without a filler.

Sample location	Element, %			Phase
	Ti	Al	V	
Point 1	1.67 ± 0.4	97.58 ± 4.6	0.75 ± 0.2	Al
Point 2	1.64 ± 0.3	97.86 ± 4.2	0.50 ± 0.6	Al
Point 3	45.78 ± 4.2	52.50 ± 1.8	1.72 ± 1.5	γ-TiAl ($L1_0$)
Point 4	40.45 ± 4.1	57.95 ± 2.1	1.60 ± 1.4	γ-TiAl ($L1_0$)
Point 5	56.77 ± 4.8	41.50 ± 1.4	1.73 ± 1.5	γ-TiAl ($L1_0$)
Point 6	51.76 ± 4.8	46.39 ± 1.6	1.85 ± 1.6	γ-TiAl ($L1_0$)
Point 7	55.43 ± 4.1	42.95 ± 1.4	1.62 ± 1.3	γ-TiAl ($L1_0$)
Point 8	88.66 ± 5.4	9.05 ± 0.4	2.29 ± 1.7	α+β Ti

areas the Ti/Al ratio varies from 40.45 / 57.95 at. % to 56.77 / 41.50 at. %. Considering the Ti-Al binary phase diagram presented by Oshnuma et al., this is the only possible phase to have formed with such a ratio [18]. However, it is important to mention that although the TiAl phase was detected by the XRD analysis other phases were also present in the sample. This means that some degree of error may by possible not so much a result of the data collection procedure, but to the poor mixing between the primary Al and Ti phases. As expected, the chemical composition of point 8, taken from the Ti64 HAZ, corresponds to the composition of the Ti64 alloy itself with 88.66 at. % Ti, 9.05 at. % Al, and 2.29 at. % V.

In order to investigate further the distribution of the chemical elements that comprise the fusion zone the image shown in Fig. 4a was investigated, and an EDS map was obtained as shown in Fig. 4b. Three distinct phases were identified by the software - Ti, Al, and V. Although the V phase was not registered during the XRD analysis its' presence in the fusion zone is not surprising since this is a key element in the chemical composition of the Ti64 alloy, which serves as a βTi stabilizer [19]. The separate dispersion of the different elements is shown in Fig. 4c. Studying the chemical dispersion of the elements it is evident that no clear pattern can be observed. The formed mixture during the welding process has a chaotic character. This somewhat confirms that hypothesis that a much larger constituent of intermetallic compounds is present in the weld seam, as compared to what was detected quantitatively by the EDS analysis.

Fig. 5a shows the macrostructure of the dissimilar joint between the Al6082T6 plate and the Ti64 one with a vanadium filler. A rectangular-shaped weld seam was formed in this case as well. A large spherical-shaped pore with a diameter of about 1 mm has formed. The reasons for this could be numerous. A possible hypothesis is the poor miscibility due to the high amount of Ti-Al binary phases that have formed during the solidification process [20]. Another is the presence of possible residual concentration of gases, possibly hydrogen or oxygen due to the high affinity of aluminium to the absorption of both [21]. Porosity during electron beam welding could also be caused by impurities on the surface of the plates [22]. The process parameters are of high importance as well. Typically, it is known that using a beam oscillation reduces the amount of porosity in electron beam welds, however, the welding speed also has a direct correlation to porosity [23]. The higher the welding speed is the higher the solidification speed is, which promotes the segregation of structures with different thermos-physical properties (intermetallic) from the base materials [23]. Either was this is a highly undesirable since theoretically that would decrease the real volume of the weld seam, reducing its mechanical properties. Zooming the area, as shown in Fig. 5b shows that multiple different zones have formed during the welding process - an Al6082T6 heat affected zone (HAZ), a clearly visible border between the Al6082T6 HAZ and the fusion zone (FZ), a fusion zone, a clearly visible border between the FZ and the Ti64 HAZ, and the Ti64 HAZ. Fig. 5c shows the microstructure of the Al6082T6 HAZ, which is comprised of many irregularly shaped pores. No visible cracks or structures of a different phase were detected. Fig. 5d shows the microstructure at the border between the Al6082T6 HAZ and the FZ, where a number of

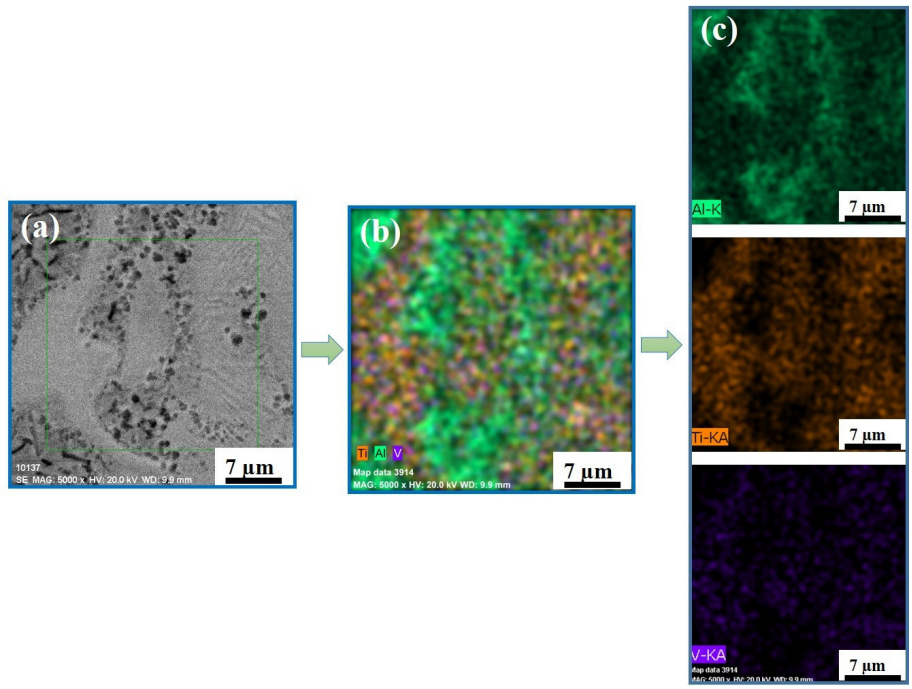

Fig. 4. SEM image of the part of the fusion zone at high magnification (a), EDS map of the investigated zone (b), particle spread across the investigated area (c) of the sample, welded without a filler.

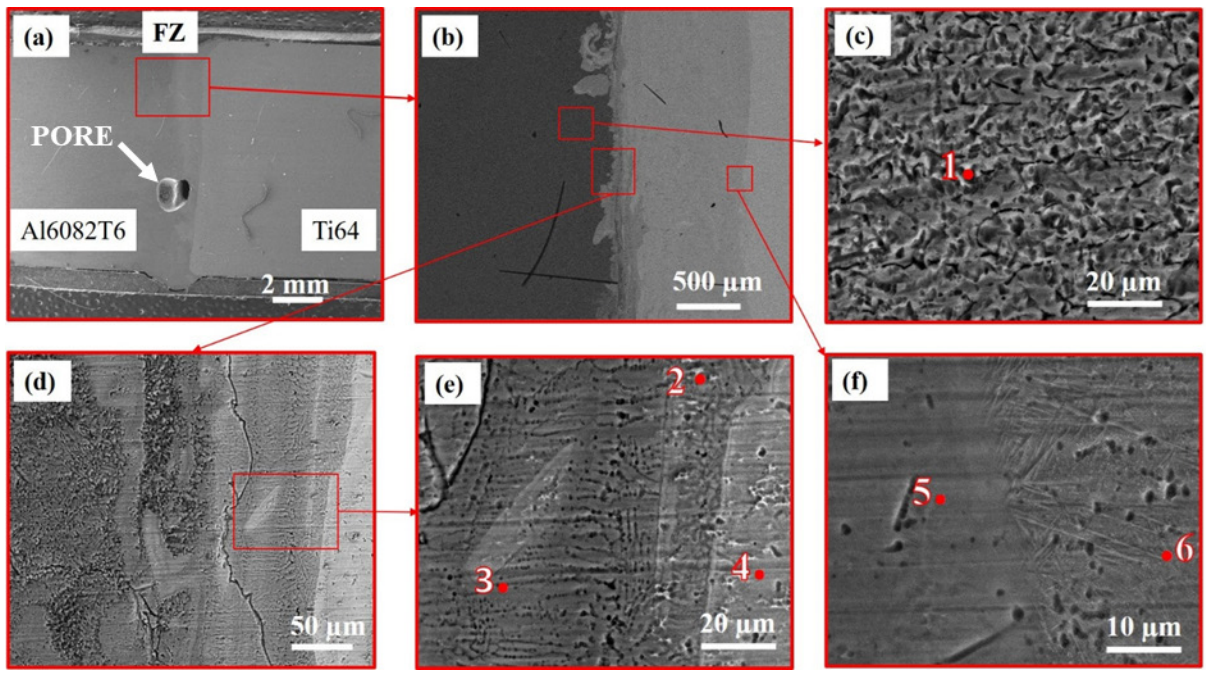

Fig. 5. SEM of the sample prepared with the V filler: (a) a macro image of the weld seam, (b) a zoomed image of the fusion zone, (c) microstructure of the aluminium HAZ, (d) microstructure of the border between the aluminium HAZ and the FZ, (e) zoomed image of the microstructure of the border between the aluminium HAZ and the FZ, (f) microstructure of the area at the border between the FZ and the Ti64 HAZ.

different structures were detected judging by the different contrast between zones, and the different orientation of the crystals. A large crack parallel to the length of the formed border has formed. A zoomed image of this zone, as shown in Fig. 5e, confirms the presence of different orientated structures with different contrast as well. Fig. 5f shows the difference between the FZ and the Ti64 HAZ. A noticeable difference in the microstructure going from one side of the image towards the other was observed. Lamellar martensitic-like structure was observed in the Ti64 heat affected zone, which is typical for this alloy.

The results of the EDS experiments of the sample prepared with a V filler were summarized in Table 3. Different zones were analysed corresponding to different microstructures. The zones are indicated in Fig. 5. Point 1 corresponds to the Al6082T6 HAZ, which unsurprisingly is comprised of 99.83 ± 4.2 at. % Al. Tiny contaminants of Ti and V were detected probably due to the sample preparation process. Points 2 and 3 correspond to the darker areas of the microstructure and apparently consist of about 55 at. % Al, 40 at. % Ti, and about 2 at. % V. Such a configuration according to the binary phase diagram [18] corresponds to the γ-TiAl ($L1_0$) phase. Points 4 and 5 belong to the lighter area of the microstructure, which consists of about 65 at. % of Ti, 35 at. % Al, and about 2 at. % V. This corresponds to the α_2-Ti_3Al ($D0_{19}$) phase. Point 6 is of the Ti64 HAZ, which is comprised of about 88 at. % Ti, 9 at. % Al, and 2 at. % V. This is typical for the structure of the Ti64 alloy.

A complementary EDS map of the fusion zone was prepared. A SEM image of the studied area is shown

Table 3. EDS results for the sample with a V filler.

Sample location	Element, %			Phase
	Ti	Al	V	
Point 1	0.07 ± 0.1	99.83 ± 4.2	0.11 ± 0.1	Al
Point 2	42.68 ± 2.9	55.65 ± 1.8	1.67 ± 1.4	γ-TiAl ($L1_0$)
Point 3	40.73 ± 2.8	57.50 ± 2.0	1.77 ± 1.6	γ-TiAl ($L1_0$)
Point 4	60.49 ± 3.1	37.49 ± 1.2	2.02 ± 1.6	α_2-Ti_3Al ($D0_{19}$)
Point 5	70.55 ± 3.4	27.09 ± 0.8	2.36 ± 1.8	α_2-Ti_3Al ($D0_{19}$)
Point 6	88.53 ± 3.7	9.39 ± 0.3	2.08 ± 1.5	α+β Ti

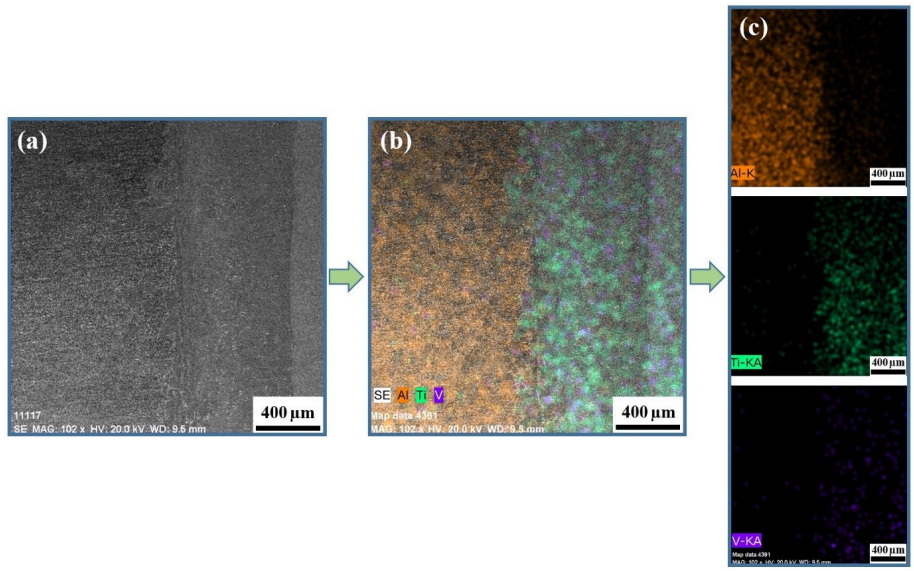

Fig. 6. SEM image of the investigated zone (a), EDS map of the investigated zone (b), particle spread across the investigated area (c) of the sample, welded with a V filler.

Table 4. Microhardness results for the samples with and without a V filler.

Sample	Microhardness, HV0.05				
	Al6082T6 plate	Al6082T6 HAZ	FZ	Ti64 HAZ	Ti64 plate
No filler	81 ± 5	96 ± 10	537 ± 43	422 ± 19	345 ± 20
V filler	70 ± 8	93 ± 12	548 ± 50	415 ± 18	365 ± 15

Table 5. Results from the performed tensile tests.

Sample	Yield strength (YS)	Ultimate tensile strength (UTS)
No filler	45 ± 4 MPa	45 ± 6 MPa
V filler	70 ± 10 MPa	71 ± 11 MPa

in Fig. 6a, and the corresponding distribution of the chemical elements is shown in Fig. 6,b. Evidently, quite high concentration of Ti was present in the fusion zone, which completely correlated to the previously made hypotheses about the predominant presence of the α_2-Ti_3Al ($D0_{19}$) phase in the volume of the fusion zone. Separate distributions of the different elements are shown in Fig. 6c, namely Al, Ti, and V. Most of the particles present in the fusion zone belong to Ti, which indicates a uniform formation and distribution of the α_2-Ti_3Al ($D0_{19}$) phase in that area.

The cross-sectional microhardness of the samples was also investigated. The results are summed up in Table 4. Al6082T6 typically has a microhardness of about 95-100 HV [24], however, in both cases it was reduced due to the heating of the material during the welding process [25]. In the case of welding without a filler the microhardness of the aluminium plate was 81 ± 5 HV0.05, and in the case of using a V filler it was 70 ± 8 HV0.05. The aluminum alloy plate has retained its microhardness in the aluminium HAZ, where it was 96 ± 10 HV0.05 and 93 ± 12 HV0.05 in both cases. The microhardness of the fusion zone in both cases was approximately the same with 537 ± 43 HV0.05, and 548 ± 50 HV0.05. Due to the noticed presence of a martensitic-like structure in the Ti64 heat affected zone an increase of the microhardness in that area compared to the base Ti64 alloy was noticed, with values of 422 ± 19 HV0.05, and 415 ± 18 HV0.05 in both cases. The rest of the Ti64 alloy plate had a typical for Ti64 microhardness of 345 ± 20 HV0.05, and 365 ± 15 HV0.05, correspondingly. Similar values of the microhardness of the Ti64 HAZ and the base material were observed by the authors of who have studied the effects of electron beam welding on Ti6Al4V. Evidently, no major changes in the values of the microhardness in the different zones of the samples prepared with and without a V filler were noticed.

The tensile properties of the samples with and without a filler were investigated. The results for the yield strength (YS) and the ultimate tensile strength (UTS) are summarized in table 5. In the case without a filler an average YS of 45 ± 4 MPa, and a UTS of 45 ± 6 MPa were reached. In the case of applying a V filler the YS value reached an average of 70 ± 10 MPa, and a UTS of 71 ± 11 MPa. An obvious increase in the tensile properties was obtained by applying the V filler. It is historically known that the ratio UTS / YS is highly descriptive of the capacity of a material to plastic deformation before failure [26].

Typically, the values for reinforcing bars should be above 1.25 to consider them as safe [27]. In the present work the UTS / YS ratio of both samples was about 1.00, which means that the samples are prone to sudden failure without a warning. This is a highly undesirable effect due to safety concerns.

CONCLUSIONS

In the present work the effect of applying a vanadium interlayer during electron beam welding of Ti64 and Al6082T6 on the structure and some mechanical properties of the obtained joints was investigated. The following conclusions can be drawn from the obtained results:

- The vanadium layer was successfully deposited using DC magnetron sputtering and then incorporated fully in the weld seam subsequently to the welding

procedure;

- Since no offset of the electron beam was applied a high quantity of titanium was incorporated in the fusion zone, which resulted in the formation of binary intermetallic such as γ-TiAl ($L1_0$), α_2-Ti_3Al ($D0_{19}$), and others;
- Due to the application of the vanadium layer a much more homogeneous distribution of the IMCs across the fusion zone was detected as compared to the sample without a filler;
- The microhardness of the studied samples was not affected by the application of the vanadium interlayer and remained approximately the same in all studied areas;
- Several defects such as pores and cracks were observed, indicating that the applied welding speed was too high, resulting in too rapid solidification;
- Despite the presence of defects in the weld seam, due to the better distribution of intermetallic phases in the sample prepared with a vanadium filler its average UTS was higher than that of the sample prepared without a filler with values of 70 ± 10 MPa and 45 ± 6 MPa, respectively.

More could be desired from the structure of the obtained samples, however, the current study shows definitive proof that the application of a vanadium layer had positive effect during electron beam welding of Ti64 and Al6082T6 without offset and with a circular beam oscillation.

Acknowledgments

This research was funded by the European Regional Development Fund within the OP "Research, Innovation and Digitalization Program for Intelligent Transformation 2021-2027", Project No. BG16RFPR002-1.014-0005 Center of competence "Smart Mechatronics, Eco- and Energy Saving Systems and Technologies".

Authors' contributions

G.K.: conceptualization, methodology, formal analysis, investigation, writing - original draft preparation, writing - review and editing, visualization; D. K.: conceptualization, methodology, formal analysis, investigation, writing - original draft preparation, visualization; M.O., V.D., A.A. B.S.: methodology, formal analysis, investigation; S. V.: conceptualization, methodology, formal analysis, investigation, writing - review and editing.

REFERENCES

1. S. Dillibabu, B. Vasudevan, M. Megaraj, A. Palanivel, R. Durvasulu, K. Manjunathan, Aluminum and its alloys in automotive and aerospace applications review, 5th International Conference on Innovative Design, Analysis and Development Practices in Aerospace and Automotive Engineering: I-DAD'22, Chennai, India, 2022, 020027. https://doi.org/10.1063/5.0139311
2. A. Heinz, A. Haszler, C. Keidel, S. Moldenhauer, R. Benedictus, W. Miller, Recent development in aluminium alloys for aerospace applications, Mat. Sci. Eng.: A, 280, 2000, 102-107. https://doi.org/10.1016/S0921-5093(99)00674-7
3. W. Miller, L. Zhuang, J. Bottema, A. Wittebrood, P. De Smet, A. Haszler, A. Vieregge, Recent development in aluminium alloys for the automotive industry, Mat. Sci. Eng.: A, 280, 2000, 37-49. https://doi.org/10.1016/S0921-5093(99)00653-X
4. J. Staley, D. Lege, Advances in aluminium alloy products for structural applications in transportation, J. Phys. IV, 3, 1993, C7-179. https://doi.org/10.1051/jp4:1993728
5. J. Hirsch, Automotive trends in aluminium-The European perspective, Proceedings of the 9th International Conference of Aluminium Alloys, Brisbane, Australia, 2004, 15-23. http://www.icaa-conference.net/ICAA9/data/papers/INV%202.pdf
6. M. Rao, K. Padal, New developments of aluminium alloys for future generation applications-A review, Fourth International Congress on Advances in Mechanical Sciences: ICAMS 2021, Hyderabad, India, 2021, 2648. https://doi.org/10.1063/5.0114421
7. F. Fernandes, J. Gonçalves, A. Pereira, Evaluation of Laser Lap Weldability between the Titanium Alloy Ti-6Al-4V and Aluminum Alloy 6060-T6, Crystals, 13, 2023, 1448. https://doi.org/10.3390/cryst13101448
8. A. Sambasiva, G. Madhusudhan, K. Satya, Microstructure and tensile properties of dissimilar metal gas tungsten arc welding of aluminum to titanium alloy, Mat. Sci. Technol., 27, 2011, 65-70.

https://doi.org/10.1179/174328409X412014
9. S. Wei, Y. Li, J. Wang, K. Liu, Use of Welding-Brazing Technology on Microstructural Development of Titanium/Aluminum Dissimilar Joints, Mat. Manuf. Process., 29, 2014, 961-968. https://doi.org/10.1080/10426914.2014.921711
10. G. Koltarski, D. Kaisheva, A. Anchev, M. Ormanova, B. Stoyanov, V. Dunchev, S. Valkov, Electron-Beam Welding of Titanium and Ti6Al4V Using Magnetron-Sputtered Nb, V, and Cu Fillers, Metals, 14, 2024, 417. https://doi.org/10.3390/met14040417
11. D. Kaisheva, G. Kotlarski, M. Ormanova, B. Stoyanov, V. Dunchev, A. Anchev, S. Valkov, Effect of Beam Power on Intermetallic Compound Formation of Electron Beam-Welded Cu and Al6082-T6 Dissimilar Joints, Eng., 6, 2025, 6. https://doi.org/10.3390/eng6010006
12. E. Akman, A. Demir, T. Canel, T. Sinmazcelik, Laser welding of Ti6Al4V titanium alloys, J. Mat. Process. Technol., 209, 2009, 3705-3713. https://doi.org/10.1016/j.jmatprotec.2008.08.026
13. S. Kuryntsev, A Review: Laser Welding of Dissimilar Materials (Al/Fe, Al/Ti, Al/Cu) - Methods and Techniques, Microstructure and Properties, Materials, 15, 2022, 122. https://doi.org/10.3390/ma15010122
14. A. Skolakova, J. Leitner, P. Salvetr. P. Novak, D. Deduytsche, J. Kopecek, C. Detavernier, D. Vojtech, Kinetic and thermodynamic description of intermediary phases formation in Ti-Al system during reactive sintering, Mat. Chem. Phys., 230, 2019, 122-130. https://doi.org/10.1016/j.matchemphys.2019.03.062
15. H. Zhang, N, Zhang, Q. Jia, D. Li, Calculation and experimentation on the formation sequence of compounds at Al/Ti interface in pure Al antioxidant coatings, Mat. Comm., 25, 2020, 101192. https://doi.org/10.1016/j.mtcomm.2020.101192
16. V. Gadakh, V. Badheka, A. Mulay, Solid-state joining of aluminum to titanium: A review, Proc. Inst. Mech. Eng., Part L: J. Mat.: Des. Appl., 235, 2021, 1757-1799. https://doi.org/10.1177/14644207211010839
17. G. Kotlarski, M. Ormanova, A. Nikitin, I. Morozova, R. Ossenbrink, V. Michailov, N. Doynov, S. Valkov, Structure Formation and Mechanical Properties of Wire Arc Additively Manufactured Al4043 (AlSi5) Components, Metals, 14, 2024, 183. https://doi.org/10.3390/met14020183
18. I. Oshnuma, Y. Fujita, H. Mitsui, K. Ishikawa, R. Kainuma, K. Ishida, Phase equilibria in the Ti-Al binary system, Acta Materialia, 48, 2000, 3113-3123 https://doi.org/10.1016/S1359-6454(00)00118-X
19. S. Huang, Q. Zhao, C. Wu, C. Lin, Y. Zhao, W. Jia, C. Mao, Effects of β-stabilizer elements on microstructure formation and mechanical properties of titanium alloys, J. All. Comp., 876, 2021, 160085. https://doi.org/10.1016/j.jallcom.2021.160085
20. M. Zhipeng, C. Wang, H. Yu, J. Yan, H. Shen, The microstructure and mechanical properties of fluxless gas tungsten arc welding-brazing joints made between titanium and aluminum alloys, Mat. Des., 45, 2013, 72-79. https://doi.org/10.1016/j.matdes.2012.09.007
21. J. Huang, N. Warnken, J. Gebelin, M. Strangwood, R. Reed, On the mechanism of porosity formation during welding of titanium alloys, Acta Materialia, 60, 2012, 3215-3225. https://doi.org/10.1016/j.actamat.2012.02.035
22. N. Gouret, E. Ollivier, G. Dour, R. Fortunier, B. Miguet, Assessment of the origin of porosity in electron-beam-welded TA6V plates, Metall. Mat. Trans. A, 35, 2004, 879-889. https://doi.org/10.1007/s11661-004-0013-z
23. B. Bandi, S. Dinda, J. Kar, G. Roy, P. Srirangam, Effect of weld parameters on porosity formation in electron beam welded Zircaloy-4 joints: X-ray tomography study, Vacuum, 158, 2018, 172-179. https://doi.org/10.1016/j.vacuum.2018.09.060
24. M. El-Shennnawy, K. Abdel-Aziz, A. Omar, Metallurgical and Mechanical Properties of Heat Treatable Aluminum Alloy AA6082 Welds, Int. J. Appl. Eng. Res., 12, 2017, 2832-2839. https://www.semanticscholar.org/paper/Metallurgical-and-Mechanical-Properties-of-Heat-AA/72f339660a038b16e752c64916c4670b9c44916c
25. P. Woelke, B. Hiriyur, K. Nahshon, J. Hutchinson, A practical approach to modeling aluminum weld fracture for structural applications, Eng. Fra. Mech., 175, 2017, 72-85. https://doi.org/10.1016/j.engfracmech.2017.02.010
26. N. Saresh, M. Pillai, J. Mathew, Investigations into the effects of electron beam welding on thick Ti-6Al-V titanium alloy, J. Mat. Process. Technol., 192, 2007, 83-88. https://doi.org/10.1016/j.jmatprotec.2007.04.048

27. Tavio, R. Anggraini, I. Raka, Agustiar, Tensile strength/yield strength (TS/YS) ratios of high-strength steel (HSS) reinforcing bars, Proceedings of the International Seminar on Metallurgy and Materials (ISMM2017): Metallurgy and Advanced Material Technology for Sustainable Development, Jakarta, Indonesia, 2018, 020036. https://doi.org/10.1063/1.5038318